npg

ORIGINAL ARTICLE

Redeployment-based drug screening identifies the anti-helminthic niclosamide as anti-myeloma therapy that also reduces free light chain production

FL Khanim[1], BAME Merrick[2], HV Giles[2], M Jankute[1], JB Jackson[1], LJ Giles[2], J Birtwistle[2], CM Bunce[1] and MT Drayson[2]

[1]School of Biosciences, University of Birmingham, Birmingham, UK and [2]Division of Immunity and Infection, University of Birmingham, Birmingham, UK

Despite recent therapeutic advancements, multiple myeloma (MM) remains incurable and new therapies are needed, especially for the treatment of elderly and relapsed/refractory patients. We have screened a panel of 100 off-patent licensed oral drugs for anti-myeloma activity and identified niclosamide, an anti-helminthic. Niclosamide, at clinically achievable non-toxic concentrations, killed MM cell lines and primary MM cells as efficiently as or better than standard chemotherapy and existing anti-myeloma drugs individually or in combinations, with little impact on normal donor cells. Cell death was associated with markers of both apoptosis and autophagy. Importantly, niclosamide rapidly reduced free light chain (FLC) production by MM cell lines and primary MM. FLCs are a major cause of renal impairment in MM patients and light chain amyloid and FLC reduction is associated with reversal of tissue damage. Our data indicate that niclosamides anti-MM activity was mediated through the mitochondria with rapid loss of mitochondrial membrane potential, uncoupling of oxidative phosphorylation and production of mitochondrial superoxide. Niclosamide also modulated the nuclear factor-κB and STAT3 pathways in MM cells. In conclusion, our data indicate that MM cells can be selectively targeted using niclosamide while also reducing FLC secretion. Importantly, niclosamide is widely used at these concentrations with minimal toxicity.

Introduction

Multiple myeloma (MM), a malignancy of differentiated B cells, remains incurable. It is characterised by >10% neoplastic plasma cells in the bone marrow, monoclonal immunoglobulin (Ig) in serum and/or urine, lytic bone lesions and fractures, anaemia and infection associated with immunodeficiency. Most patients also develop renal impairment (RI) at some point during their disease with 30% presenting with RI at diagnosis.[1–3] Several studies have confirmed that RI is associated with poor prognosis in MM with a median survival of <2 years.[4–6] The causes of RI in myeloma are multifactorial but predominantly attributable to nephrotoxic free Ig light chains (FLC) secreted from the myeloma cell clone.[7] Reversal of RI with high-dose dexamethasone (DEX)[8] combined with bortezimib is a recommended treatment for MM patients with any grade of RI[3] and induces rapid reduction in serum FLC levels and associated renal recovery.[9]

Improvements in survival outcomes in MM have been achieved in the last three decades, especially in younger patients. The development of high-dose melphalan with autologous stem cell transplant for younger (<65 years) fitter patients[10–12] and new therapies incorporating combinations of corticosteroids and conventional chemotherapy agents with immunomodulatory drugs (thalidomide and lenalidomide), and proteasome inhibitors (bortezomib) have increased median survival to 4–5 years.[13–15] However, high-dose chemotherapy and autologous stem cell transplant are not suitable for elderly frail patients due to significant toxicities. Approximately 85% of myeloma patients are >60 years of age with a median age at presentation of ~70 years and median survival has remained 2–3 years in the over 70 cohort. Relapse with resistant disease is a major cause of death in MM and although some agents used as initial therapy (including thalidomide, lenalidomide and bortezomib) have shown activity and some improved outcomes in patients with relapsed or refractory MM,[16–19] these responses are usually of limited duration.[20] Consequently, effective non-toxic therapies that provide either a cure or durable disease control with symptomatic relief for elderly or relapsed/refractory patients are urgently needed.

An alternative to new drug development is drug repositioning/ redeployment, the testing of existing compounds for efficacy in diseases other than those the drug is normally used to treat. The use of thalidomide in myeloma and ATRA in acute promyelocytic leukaemia are good examples of this. This approach bypasses a significant proportion of the cost of developing a drug, the average pre-approval cost of developing a drug is over 800 million dollars,[21,22] and increases the speed that potentially therapeutic discoveries in the laboratory can be translated into the clinic. We have used a drug redeployment/reprofiling strategy to screen a library of 100 off-patent drugs/agents, at clinically relevant peak serum concentrations, for anti-myeloma activity against myeloma cell lines in vitro. The screen identified niclosamide, a broad-spectrum anti-helminthic, as having potent anti-myeloma activity against myeloma cell lines. Importantly, niclosamide reduced the production of free light chain production by both myeloma cell lines and primary myeloma cells in vitro. These data highlight the therapeutic potential of niclosamide in the treatment of MM and also other paraproteinaemias.

Materials and methods

Drugs

All drugs were purchased from Sigma Aldrich (Dorset, UK). Stocks were prepared at $10\,000\times$ reported peak serum concentrations and stored at $-20\,^\circ$C. Niclosamide (3.2 mM), prednisolone (716 mM)[23] and chlorambucil (16.2 mM)[24] were

prepared in ethanol. Melphalan (20 mM),[25] DEX (4.33 mM),[26] cyclophosphamide (2 M),[27] thalidomide (109 mM)[28,29] and methotrexate (10 mM)[30] were prepared in dimethyl sulfoxide.

Cell culture and drug treatments
JJN3, H929 and U266 cell lines were purchased from ATCC. L363, OPM-1, RPMI 8226, LME-1, UM-1 and UM-3 were a kind gift from Prof Pranab Das (University of Amsterdam, the Netherlands). Stock cultures were maintained in RPMI 1640 medium with L-glutamine supplemented with 10% v/v heat inactivated fetal bovine serum and penicillin (100 units/ml)/ streptomycin (100 µg/ml) (all from Gibco, Invitrogen Ltd, Paisley, UK) at 37 °C with 5% CO_2. Cells were passaged every 2–3 days maintaining cell densities between $0.5–2 \times 10^6$ cells/ ml. Drug treatments in 96-well plate assays were performed using 2×10^4 cells/well in 200 µl or at 0.5×10^6 cells/ml in 4 ml media in flasks. Appropriate volumes of dimethyl sulfoxide and/ or ethanol were added as solvent controls to control treatments.

Measurement of cell viability
Cell viability was measured using one of three methods as specified in the text. Numbers of viable cells in triplicate wells of 96-well plates were determined using CellTiter-Blue reagent according to manufacturer's instructions (Promega, Southampton, UK). Viable cell counts were performed using manual counts, or by flow cytometry on a BD FACSCalibur utilising Cell Quest Pro software (BD, Oxford, UK), viable gates and fluorescent Cytocount beads (Dako, Ely, UK).

Assessment of apoptosis by annexin V, cell cycle and caspase cleavage
All analyses were carried out by flow cytometry on a BD FACSCalibur utilising Cell Quest Pro software (BD). Apoptosis was assessed using an annexin V FITC kit (BD) and a pan-caspase assay kit (CaspaTag, Chemicon, Millipore, Watford, UK) according to manufacturer's instructions. Cell cycle was analysed by resuspending cell pellets from 500 µl cell suspensions in 500 µl cell cycle buffer (30 µg/ml proteasome inhibitor, 0.1 mM sodium chloride, 1% sodium citrate, 1% Triton X100) and incubating at 4 °C for 4 h before flow cytometric analysis.

Assessment of reactive oxygen species and mitochondrial superoxide (mitosox)
MitoSOX Red (Molecular Probes, Invitrogen, Paisley, UK) was used to assess mitosox. PBS-washed cells were resuspended in 200 µl 37 °C PBS containing 5 µM MitoSOX Red, incubated at 37 °C for 10 min and then analysed by flow cytometry (emission wavelength 580 nm). Reactive oxygen species (ROS) was measured using carboxy-H_2DCFDA (5-(and-6)-carboxy-2′,7′-dichlorodihydrofluorescein diacetate; Molecular Probes). Cells were treated with drugs at 37 °C and 10 µM carboxy-H_2DCFDA (Molecular Probes) added to 0.5 ml cell suspension for the final 45 min. Following incubation, cells were analysed by flow cytometry (emission wavelength 517–527 nm) (BD FACSCalibur and BD Cell Quest software). For real-time measurement of mitosox and ROS generation, cells were pre-labelled with MitoSOX Red or carboxy-H_2DCFDA. Baseline ROS or mitosox was measured by flow cytometry, the drug was added and then measurements were taken at specified time intervals.

Measurements of mitochondrial membrane potential (Δψ)
5,5′,6,6′-tetrachloro-1,1′,3,3′-tetraethylbenzimidazolylcarbo-cyanine iodide (JC-1; Sigma Aldrich) was dissolved at 1 mg/ml in dimethyl sulfoxide and stored at −20 °C. Following treatment, cells were incubated with 2.5 µg/ml JC-1 at 37 °C for 30 min, before analysis by flow cytometry. TMRE (tetramethylrhoda-mine, ethyl ester) was prepared as a 20 µM stock in dimethyl sulfoxide. Cells were labelled in media with 10 nM TMRE for 10 min and then analysed by flow cytometry.

Measurement of respiration rates
A Clark oxygen electrode (Rank Brothers Ltd, Cambridge, UK) was used to measure respiration rates according to the manufacturer's instructions and data recorded using a chart recorder. Briefly, the incubation chamber was filled with 1300 µl fresh RPMI 1640 media with supplements and the readout calibrated at 100% O_2 at 37 °C. Cells (50×10^6) in 200 µl of RPMI 1640 media with supplements were injected into the incubation chamber and basal respiration rate recorded until 60% O_2 remained. Subsequently, niclosamide (3.2 µM) or the classical oxidative phosphorylation uncoupler p-trifluoro-methoxy carbonyl cyanide phenyl hydrazone (Sigma) (6.7 µM) was injected into the incubation chamber and the respiration rate was recorded until 0% O_2 was achieved. Gradients of oxygen depletion were measured and respiration rates calcu-lated as µmol molecular $O_2/10^6$ cells/min assuming 100% $O_2 = 0.257$ µmol O_2/ml at 37 °C.

FLC measurement in the supernatants of MM cells
FLC levels in the supernatants of MM cell lines were measured using mouse monoclonal antibodies specific for free Igκ or λ light chains (Freelite assay, Binding Site, Birmingham, UK[31]) in a Bio-Plex suspension array system (Bio-Plex HTF System, Bio-Rad, Hercules, CA, USA). Cells of interest were washed with media, seeded in fresh media into 96-well plates at a density of 50×10^3 cells/well, treated with appropriate agents and incubated at 37 °C with 5% CO_2. DEX served as a positive control as it has been shown to decrease the production of FLCs.[32,33] After incubation, supernatant from 150 µl of cells was used to determine light chain production. Cell viability was assessed in a second 150 µl aliquot of cells using Cytocount beads (Dako) and flow cytometry. Ig production was normalised to viable cell number.

Western blot analyses
Cells were lysed in RIPA buffer (1% v/v NP40, 0.5% w/v sodium deoxycholate, 0.1% w/v 10% SDS, protease inhibitors) and 30 µg proteins separated by SDS-polyacrylamide gel electro-phoresis. Proteins were transferred to Immobilon-P membrane (Millipore Corp., Bedford, MA, USA) and probed with 1/1000 dilution of anti-LC3 antibody (Novus Biologicals, Cambridge, UK). Detection was by anti-mouse-horse radish peroxidise (Sigma) diluted 1/1000 and ECL using Supersignal Dura Chemiluminescent substrate (Pierce, Rockford, IL, USA). Anti-β-actin antibody (Sigma) diluted 1/25 000 and anti-mouse-horse radish peroxidise secondary at 1/25 000 were used as loading control. STAT3 levels were measured using mAb anti-STAT3 (BD) and anti-pY705-STAT3 (Cell Signalling Technologies, Hitchin, UK) antibodies.

Real-time PCR quantification
Reactions were performed using an ABI Prism 7700 sequence detector (Applied Biosystems, Life Technologies Ltd, Paisley, UK). Gene-specific primers were synthesised by Sigma Genosys

(Haverhill, UK) and probes by Eurogentec Ltd (Southampton, UK). Igκ forward primer: 5′-CACACTGGCCTCCGATCAC-3′, Igκ reverse: 5′-TGCAGCCACAGTTCGTTTAATC-3′; Igλ forward: 5′-CCACCAAACCCTCCAAACAG-3′, Igλ reverse: 5′-GGGC GTCAGGCTCAGGTA-3′ (κ probe: 6-FAM-TTCGGCCAAGGG ACACGACTG-TAMRA; λ probe: 6-FAM-CAACAACAAGTAC GCGGCCAGCAG-TAMRA). Each reaction contained 900 nM of gene specific 5′ and 3′ primers, 1 × Mastermix (Eurogentec), 125 nM gene-specific probe (5′-6′-FAM, 3′-TAMRA labelled) and cDNA in a total volume of 20 μl. Internal standard control 18S ribosomal RNA reactions contained 50 nM 18S 5′ and 3′ primers, 200 nM 18S probe (5′-VIC, 3′-TAMRA labelled; Applied Biosystems) and cDNA in a total volume of 20 μl. Cycle conditions for the thermal cycler were denaturation at 95 °C and annealing and elongation at 60 °C for 1 min, repeated 44 times.

Jenner Giemsa staining of cytospin cell preparations
Cytospins were prepared from 75 to 100 μl of culture. Slides were air dried, methanol fixed and stained, 5 min with Jenner staining solution (VWR, Lutterworth, UK) diluted 1/3 in 1 mM sodium phosphate buffer pH 5.6, washed with distilled water and then 10 min with Giemsa stain (VWR) diluted 1/20 in 1 mM sodium phosphate buffer, pH 5.6. Slides were dried and then mounted onto coverslips using DePex (VWR).

Statistics
Data were analysed using SPSS v15 (IBM, Portsmouth, UK) and the non-parametric Mann–Whitney U-test or analysis of variance. Unless stated in the legend, the statistics shown in figures are all compared to control cultures.

Results

Drug screening identifies niclosamide as being as efficient as common chemotherapeutics at killing myeloma cells
The viability of three myeloma cell lines, H929, JJN3, U226, was assessed following 72 h treatments with a panel of 100 drugs (Drug Library FMC1) (Supplementary Figure 1). The library was compiled by selecting oral, off-patent drugs of low toxicity from all 15 chapters of the British National Formulary. Importantly, each drug was used at the maximum peak serum concentrations achieved as reported in the literature following use for standard clinical indications. Of the 100 drugs, niclosamide, an anti-helminthic, demonstrated potent anti-proliferative activity against all three myeloma cell lines (Supplementary Figure 1). The anti-proliferative actions of niclosamide proved to be as effective as, if not more than, reported peak serum concentrations of several common chemotherapy (oral methotrexate, chlorambucil) and anti-myeloma drugs (prednisolone, cyclophosphamide, DEX and thalidomide) included in the library (Figure 1a).

Using a larger panel of eight myeloma cell lines and four primary MM bone marrow samples (MM1-4), the anti-proliferative effect of niclosamide at peak serum concentration (3.2 μM) was compared with the anti-myeloma drug combinations of melphalan/prednisolone/thalidomide (MPT) and cyclophosphamide/thalidomide/DEX (CTD). As shown in Figure 1b, the drug combinations had variable anti-proliferative activity against the eight cell lines with MPT being the more potent. In contrast, all the cell lines displayed marked sensitivity to 3.2 μM

niclosamide. All of the four primary MM samples demonstrated sensitivities to niclosamide that were at least equivalent to MPT if not better, with CTD being the least potent in these *in vitro* assays. All the cell lines and primary MM samples demonstrated dose-dependent responses to niclosamide, with 1 μM niclosamide being as potent *in vitro* as CTD and MPT in many of the myeloma cell lines (Supplementary Figures 2 and 3). The dose and time dependency of the niclosamide response of JJN3, U266 and H929 cells are shown in Figure 1c. As early as 18 h after addition of drug, significant loss of viability was observed with as little as 1 μM niclosamide (H929: 69.0%, JJN3: 72.1%, U266: 74.9%, $P<0.05$). These decreases in viability became more apparent at 42 h in H929 and JJN3 (H929: 45.9%, JJN3: 32.7%, U266: 77.7%, $P<0.05$) and in all three lines at 66 h (H929: 8.4%, JJN3: 3.5%, U266: 57.1%, $P<0.05$). Importantly, niclosamide at doses that impacted significantly on MM cell survival (0.5 and 1.0 μM) did not affect the viability of normal donor PBMCs, with no affect on the number of monocytes, B lymphocytes, C4 and CD8 T cells over a 7-day period (Supplementary Figure 4). These data indicate that all three myeloma cell lines were sensitive to doses of niclosamide that are likely to be clinically achievable using standard treatment regimens and that are unlikely to impact upon normal healthy PBMCs.

The anti-myeloma activity of niclosamide is associated with markers of apoptosis and autophagy
Flow cytometry analysis identified a clear dose-dependent increase in annexin V positive and annexin V/propidium iodide co-positive cells in the three myeloma cell lines analysed (Figure 2a). In parallel, analysis of caspase activity using a fluorescent pan-caspase assay and flow cytometry identified a similar dose-dependent increase in caspase activity following niclosamide treatment for 48 h (Figure 2b). These data indicate that niclosamide treatment induced apoptosis in myeloma cell lines. However, despite the accumulation of annexin V positive cells following treatment with niclosamide and the activation of caspases, no major increase in the cell cycle sub-G1 fraction (M3), which is indicative of DNA cleavage and cellular fragmentation during apoptosis, was observed (Figure 2c). Similarly, morphological analysis of cytospin preparations of niclosamide-treated cells did not identify significant numbers of cells with classical hallmarks of apoptosis including condensed fragmented nuclei and shrunken cells (Figure 2d). Instead, the cells appeared enlarged, vesicular and collapsed upon preparation of the cytospins suggesting fragile plasma membranes. As niclosamide has been demonstrated to induce autophagy in MCF-7 cells,[34] we measured the levels of the autophagosome-associated protein LC3-II in JJN3 cells treated with solvent control or niclosamide for 24 h. Western blot analysis identified a clear increase in LC3-II levels in niclosamide-treated cells consistent with induction of autophagy (Figure 2e). Thus niclosamide induces cell death in myeloma cells with markers of both apoptosis and autophagy.

Inhibition of FLC production
Given the clinical importance of reducing FLC levels for reducing renal damage, we measured the impact of niclosamide on FLC production. All myeloma cell lines were initially assessed for their FLC secretion. Four lines were identified as Igκ secretors (JJN3, UM3, LME-1 and H929) and three as Igλ secretors (L363, RPMI 8226 and U226) and two were non-secretors (OPM1 and UM1) (Supplementary Figure 5). JJN3 and UM3 cell lines were selected as strong Igκ secretors and L363
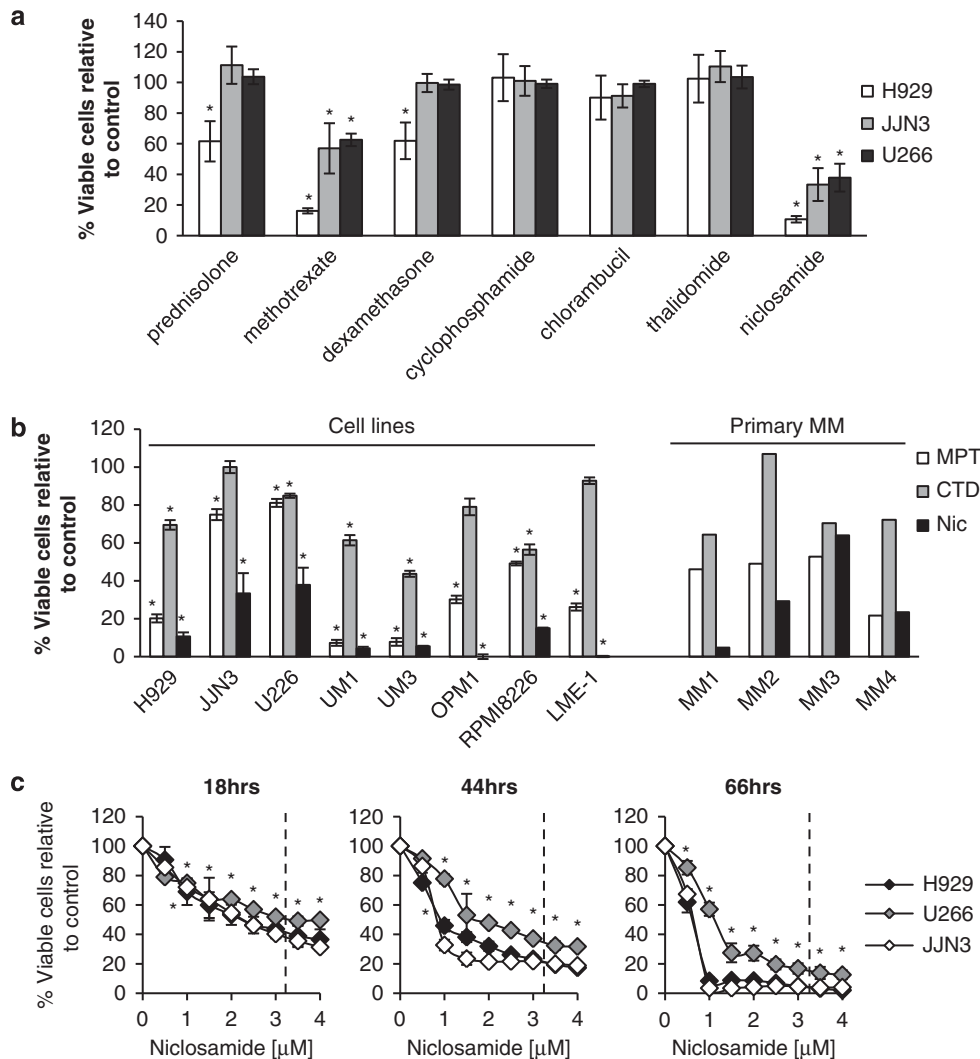
Figure 1 Niclosamide has potent anti-myeloma activity at peak serum concentrations. (**a**) H929, JJN3 and U266 cells were treated with peak serum concentrations of a library of 100 drugs for 72 h. Viability was assessed using CellTiter Blue (Promega) and calculated as percentage of control. Myeloma cell line responses to the commonly used anti-myeloma therapeutics prednisolone (71.6 μM), oral methotrexate (1 μM), dexamethasone (0.43 μM), cyclophosphamide (200 μM), chlorambucil (1.62 μM), thalidomide (10.9 μM) and the anti-helminthic niclosamide (3.2 μM) are shown. Data are the mean of three experiments ± s.e.m. (**b**) A panel of eight myeloma cell lines were treated for 72 h with two currently used anti-myeloma combinations MPT (melphalan 10 μM/prednisolone 71.6 μM/thalidomide 10.9 μM) or CTD (cyclophosphamide 200 μM/thalidomide 10.9 μM/dexamethasone 0.43 μM), and niclosamide at 3.2 μM. Viability was assessed using CellTiter Blue (Promega) and calculated as percentage of control. Data are the mean of a minimum of three experiments ± s.e.m. Primary myeloma bone marrow samples (MM1-4) were also treated as for the cell lines but for 48 h. Viability was assessed by CD138/38 and annexin V staining and flow cytometry. (**c**) H929, JJJN3 and U266 cells were treated with different doses of niclosamide at different timepoints and viability assessed by flow cytometry using viable cells gates and Cytocount beads. Data are the mean of three experiments ± s.e.m.; *$P < 0.05$.

and RPMI 8226 as strong Igλ secretors. FLC levels in cell supernatant was assessed following treatment with niclosamide and compared with 5 μM DEX. As shown in Figure 3a, 18 h treatment with niclosamide at either 0.5 or 1 μM decreased Igκ/λ secretion in all cell lines tested by between 15–60%. Furthermore the ability of niclosamide to reduce Igκ/λ secretion compared favourably with that of 5 μM DEX, which reduced secretion only in UM3 and RPMI 8226 cells by ~20% (Figure 3a). To determine whether the reduction in extracellular FLC was as a result of reduced transcription, translation or export, we measured the intracellular protein and mRNA levels of Ig using indirect intracellular flow cytometry and quantitative real-time PCR, respectively. Following 18 h treatment with 1 μM niclosamide significant decreases were observed in intracellular

FLC protein levels in both cell lines analysed (JJN3: Igκ: 38% and L363: Igλ: 23%, $P < 0.05$) (Figure 3b). This correlated with a significant (~20%) reduction in Igκ mRNA levels in JJN3 suggesting reduced FLC secretion was due in part to transcriptional regulation by niclosamide (Figure 3c). In contrast, Ig mRNA levels in the other lines were variable with both decreases and increases observed in response to niclosamide or DEX (Figure 3c). Importantly, niclosamide (1 μM) also reduced Ig protein levels in the supernatant of 6/9 primary myeloma cells after 18 h. Interestingly, 5/5 Igκ myelomas had reduced levels of FLC whereas only 1/4 of the Igλ myelomas responded (Figure 3d). The drug combinations of MPT also reduced Ig secretion in 5/9 primary MM and CTD in 5/9 samples but not to the same extent as niclosamide (Figure 3d).
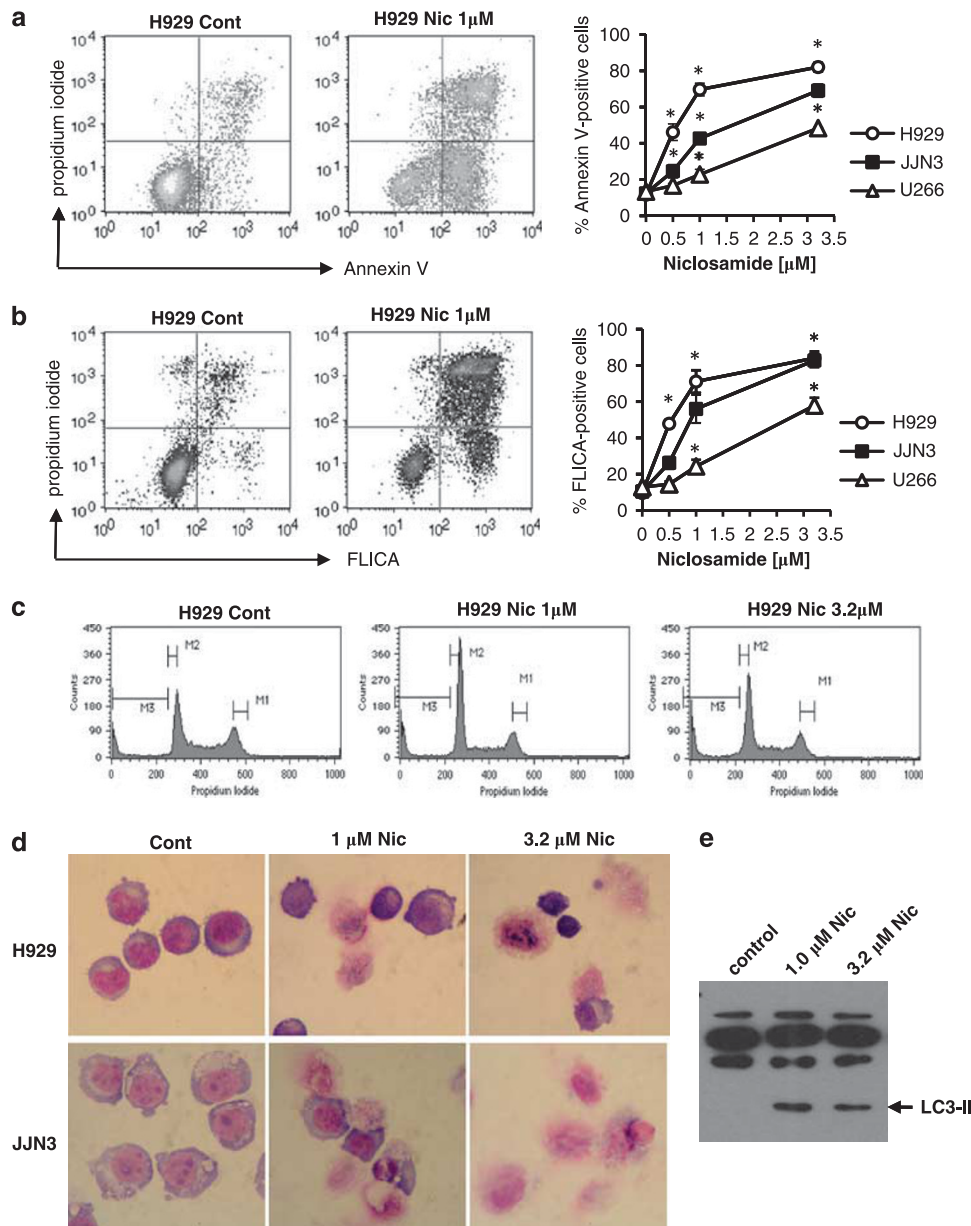
Figure 2 Niclosamide-treated myeloma cells die with markers of apoptosis and autophagy. H929, JJN3 and U226 were treated with different concentrations of niclosamide (Nic) for 48 h. Cells were analysed by flow cytometry for (**a**) annexin V/propidium iodide positivity (**b**) and caspase activity using Caspatag assay according to manufacturer's instructions. Data shown are the mean of three experiments ± s.e.m. Representative dotplots are shown for each assay; *$P < 0.05$. (**c**) Cell cycle was analysed by staining cells with propidium iodide and flow cytometry after treatment with Nic for 24 h. Representative histograms are shown for H929 cells. (**d**) Representative images are shown of Jenner/Giemsa-stained cytospins from H929 and JJN3 cells treated with solvent control or Nic for 48 h. (**e**) A volume of 30 μg total protein from JJN3 cells treated with Nic for 24 h was immunoblotted for LC3-II protein. Image shown is representative of $n = 2$ experiments.

Niclosamide induces a loss of mitochondrial membrane potential and uncouples oxidative phosphorylation in myeloma cells

Uncouplers of oxidative phosphorylation (OXPHOS) function by uncoupling the electron transport chain from ATP production, usually by increasing the proton permeability of the mitochondrial membrane thereby decreasing the proton electrochemical potential (Δp). These results in a compensatory increase in respiration rate as cells attempt to re-establish the Δp. Classical OXPHOS uncouplers include p-trifluoromethoxy carbonyl cyanide phenylhydrazone (FCCP) and carbonyl cyanide m-chlorophenyl hydrazone (CCCP), which are lipid-soluble weak acids. As, niclosamide is a weak acid and has been shown to uncouple OXPHOS in tapeworms[35] and human cells,[36,37] we tested for this activity in myeloma cells. Treatment of H929 and JJN3 myeloma cells with niclosamide resulted in loss of mitochondrial membrane potential (Δψ) as measured using the Δψ sensitive dyes JC-1 and TMRE (Figures 4a and b). Loss of Δψ was rapid being detected within 1 min using TMRE (Figures 4b and c). Loss of Δψ in niclosamide-treated cells was further confirmed using the Δψ-sensitive mitochondrial stain Mitotracker Red (data not shown). A concomitant increase in respiration rate following niclosamide-induced loss of Δψ was observed in all myeloma cell lines tested, to a similar extent as
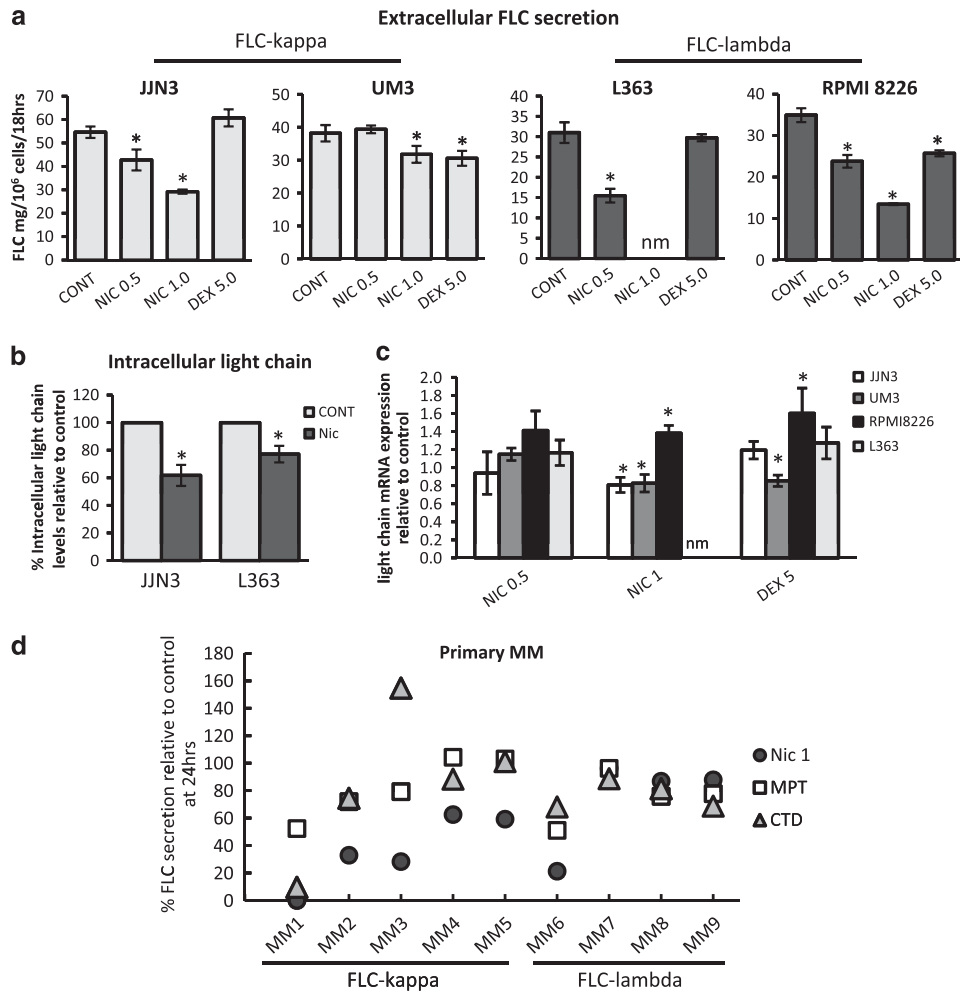
Figure 3 Niclosamide reduces FLC from myeloma cell lines and primary MM samples. (**a**) MM cell lines were treated in 96-well plates for 18 h with either solvent control, 0.5–1.0 μM niclosamide or 5 μM dexamethasone. Supernatants were harvested and FLC measured using FreeLite assay. FLC secretion was normalised for cell viability (data not shown). Nm = not measured as there was significant loss of viability. Data shown are the mean of $n = 3$ experiments ± s.e.m. (**b**) JJN3 and L363 cells were treated for 18 h with either solvent control or 1.0 μM niclosamide. Cells were washed, fixed and permeabilised and intracellular Ig detected using indirect staining and flow cytometry. Isotype matched control antibodies were used to control for non-specific binding. Data shown are the mean of $n = 3$ experiments ± s.e.m. (**c**) Ig mRNA levels were measured after 18 h treatment using quantitative real time PCR and normalised to 18S internal standards. Data shown are the mean of $n = 4$ experiments ± s.e.m.; $P < 0.05$. (**d**) Primary MM bone marrow-derived total mononuclear cells were treated in 96-well plates for 18 h with MPT (melphalan 10 μM/ prednisolone 71.6 μM/thalidomide 10.9 μM) or CTD (cyclophosphamide 200 μM/thalidomide 10.9 μM/dexamethasone 0.43 μM), or niclosamide at 1 μM. The supernatant was harvested and FLC levels measured using Luminex analysis. *$P < 0.05$.

that observed with the control uncoupler FCCP (Figure 4d and Supplementary Figure 6) with increased respiration observed within 5 s of addition of the drug. These data indicate that the mitochondria are a major target for niclosamide in myeloma cells.

Generation of mitochondrial superoxide correlates with loss of cell viability

We next measured generation of ROS using carboxy-H$_2$DCFDA and mitochondrial superoxide using MitoSOX Red and flow cytometry. JJN3 and H929 myeloma cells were labelled with each dye, baseline readings were taken using flow cytometry and then after the addition of 3.2 μM niclosamide at the times shown in Figure 5a. There was a rapid time-dependent increase in mitochondrial superoxide generation in both

cell lines, evident in H929 cells within 15 s of the addition of niclosamide and within 60 s in JJN3 cells (Figure 5a). The levels of mitochondrial superoxide continued to increase significantly during the 20 min of the experiment. In contrast, there was a small initial increase in ROS levels (∼2 fold) after the addition of niclosamide to the cells and then no further elevation over the duration of the experiment (Figure 4a).

The induction of mitochondrial superoxide was both niclosamide dose and time dependent (Figure 5b). In all three cell lines, albeit with different kinetics, niclosamide at concentrations as low as 1 μM was able to induce significant increases in mitochondrial superoxide. In JJN3 and H929 this increase occurred within 18 h whereas in U266, which is a much slower growing line, the increase was seen later (Figure 5b). Analysis of other ROS species using carboxy-H$_2$DCFDA identified no
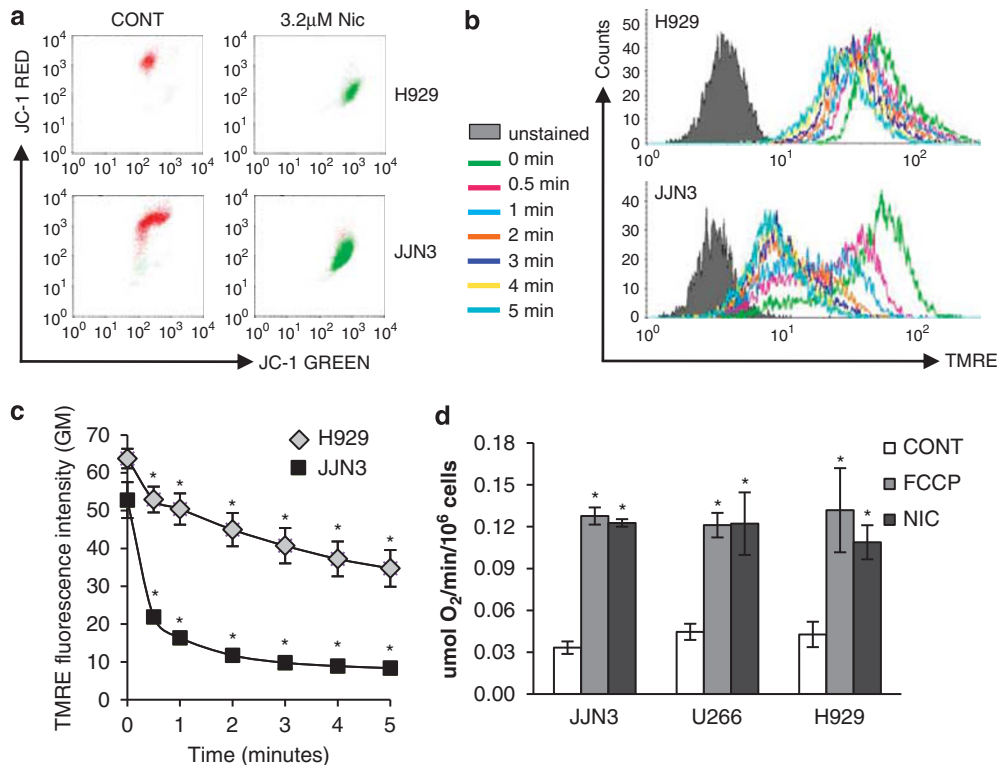
Figure 4 Niclosamide treatment results in loss of mitochondrial membrane potential (Δψ) and an increase in respiration rate. (**a**) Myeloma cells treated with niclosamide for 4 h were stained with JC-1 and analysed by flow cytometry. Red is indicative of cells with polarised mitochondrial membranes. Green staining indicates cells that have lost Δψ. Data shown is representative of $n = 3$ experiments. (**b**, **c**) H929 and JJN3 cells were prestained with 10 nM TMRE and baseline fluorescence intensity (geometric mean GM) determined by flow cytometry. Niclosamide (3.2 μM) was added and readings taken at 15, 30 s and every minute for 5 min. Representative histograms (**b**) are shown together with mean data (**c**) from $n = 4$ experiments ± s.e.m. (**d**) Respiration rate in 5×10^7 myeloma cells was measured using a Clark oxygen electrode. Baseline respiration rate was established as μmol O_2/min/10^6 cells before the addition of either 3.2 μM niclosamide or 6.7 μM *p*-trifluoromethoxy carbonyl cyanide phenylhydrazone (FCCP). Representative plots are shown together with a histogram of mean data from a minimum of $n = 4$ experiments ± s.e.m.; *$P < 0.05$.
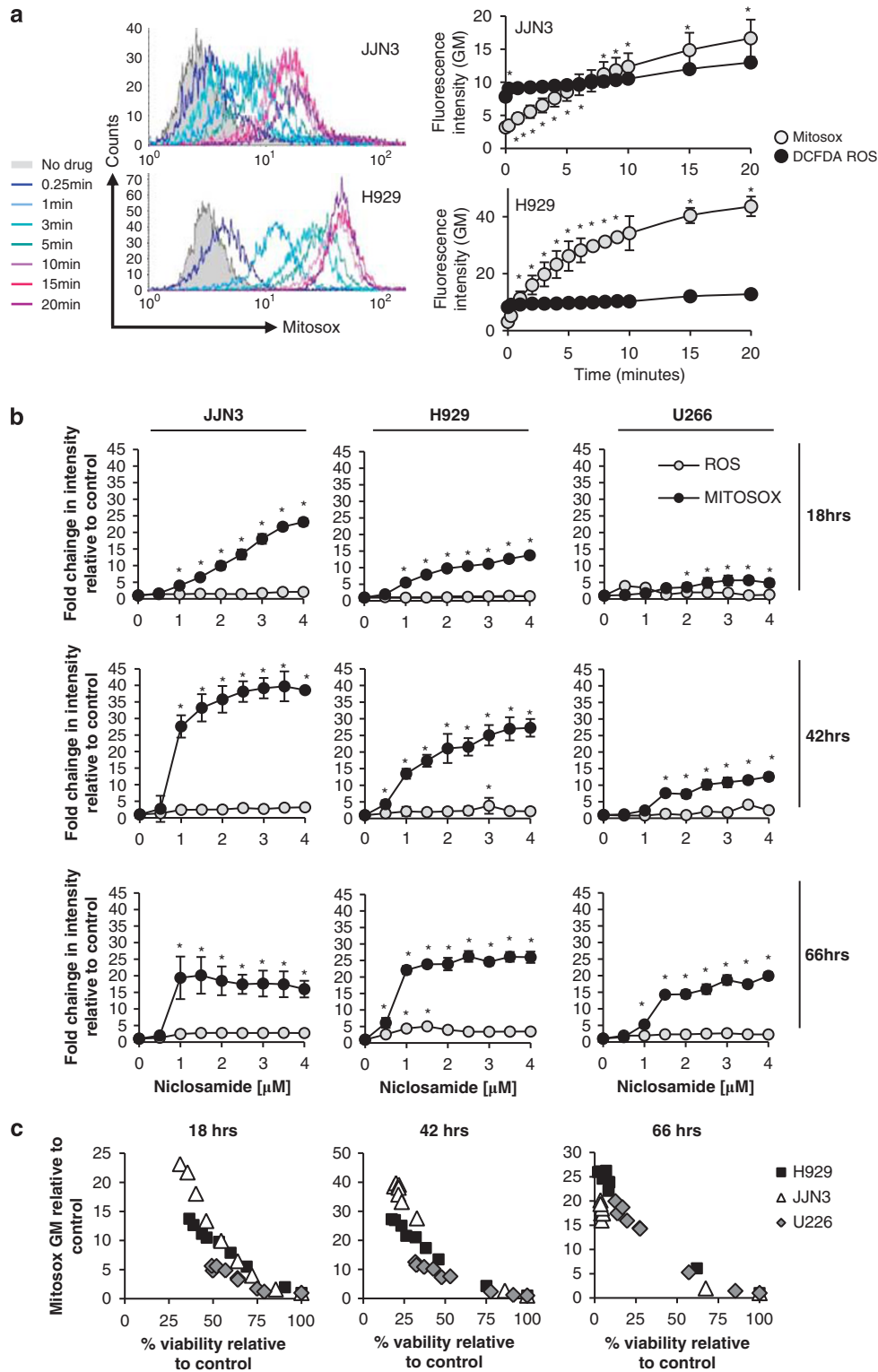
significant increase at any concentration of niclosamide used or at any of the timepoints analysed (Figure 5b) demonstrating that mitochondrial superoxide is the main ROS species generated. Cell viability was also assessed in parallel and demonstrated a strong negative correlation with mitochondrial superoxide generation (Figure 5c). Taken together these data strongly implicate that the generation of mitochondrial superoxide mediates the cytotoxicity of niclosamide against myeloma cell lines.

Niclosamide regulates multiple cellular pathways important for myeloma cells

Niclosamide has been demonstrated to regulate nuclear factor-κB (NF-κB)[38] and STAT3 signalling.[39] Both of these pathways are important players in myeloma pathogenesis and development of chemoresistance.[40–42] We treated UM3 cells with 1 μM niclosamide for 2 h and then stimulated them for 15 min with 100 ng/ml tumour necrosis factorα (TNFα). Sub-cellular localisation of the p65 NF-κB subunit was assessed using immunofluorescence staining and fluorescence microscopy. As can be seen in Figure 6a, TNFα treatment resulted in nuclear localisation of the p65 NF-κB subunit. This nuclear localisation was significantly inhibited by niclosamide treatment indicating that niclosamide can regulate the canonical NF-κB pathway in myeloma cells. It has also been shown that NF-κB signalling is essential for mediating Igκ, but not Igλ, FLC transcription,[43]

which may explain the reduction of Igκ mRNA in JJN3 and UM3 MM cells and the preferential reduction of Igκ mRNA in primary MM cell described above (Figure 3c). Hence, we treated JJN3 cells with either niclosamide (1 μM), TNFα (10 ng/ml) or the combination for 18 h and measured the Igκ mRNA levels and protein secretion. As demonstrated previously (Figure 3c), niclosamide reduced Igk mRNA levels ∼20% from controls. Co-treatment with TNFα abrogated the effects of niclosamide (Figure 6b). Importantly, TNFα was not able to restore FLC secretion from niclosamide-treated JJN3 cells (Figure 6c) indicating that niclosamide predominantly acts post-transcriptionally in reducing FLC levels thereby explaining its activity against both Igκ and Igλ secretors.

STAT3 is an important anti-apoptotic pathway in myeloma and is activated by interleukin 6, which is induced by NF-κB.[44] Niclosamide has been shown to be a small molecule inhibitor of STAT3 specifically preventing phosphorylation at tyrosine 705 (Y705) in a number of haematological malignancies.[39] Total STAT3 and STAT3 pY705 levels were measured in JJN3 cells pre-treated with 1 or 2 μM niclosamide for 2 h before activation of the STAT3 signalling pathway with interleukin 6 for 15 min. As can be seen in Figure 6d, niclosamide inhibited interleukin 6-induced phosphorylation of STAT3 Y705 phosphorylation in a dose-dependent manner with 2 μM completely inhibiting detection of phosphorylated Y705. Hence, niclosamide may induce cell death in myeloma cells in part by inhibiting STAT3 activation.
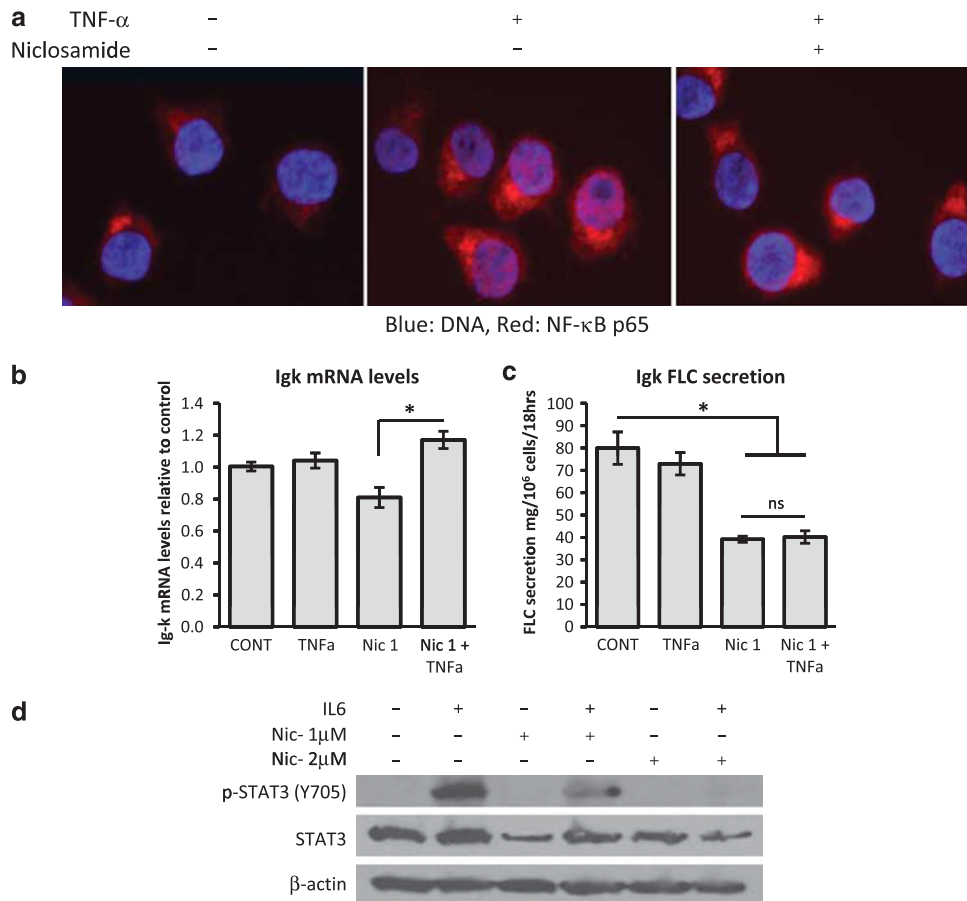
Figure 5 Generation of mitochondrial superoxide correlates with niclosamide anti-myeloma activity. (**a**) JJN3 and H929 cells were stained with MitoSOX Red or carboxy H_2DCFDA (Molecular Probes) and analysed by flow cytometry. Baseline was set before the addition of 3.2 μM niclosamide and measurements taken at regular time intervals. Histograms show representative MitoSOX Red data and line graphs show mean data from $n = 3$ experiments ± s.e.m. for both MitoSOX Red and ca-H_2DCFDA for JJN3 and H929 cells. (**b**) Myeloma cell lines H929, JJN3 and U266 were treated with different doses of niclosamide for 18, 42 or 66 h. Aliquots of cells were removed, stained with MitoSOX Red or carboxy H_2DCFDA and analysed by flow cytometry. Data are shown as intensity of fluorescence (geometric mean (GM)) relative to solvent-treated controls and is the mean of $n = 3$ experiments ± s.e.m. (**c**) Viability was also assessed at 18, 42 and 66 h by flow cytometry of fixed cells using viable gates and Cytocount beads and is plotted against relative MitoSOX Red fluorescence intensity to demonstrate the relationship between niclosamide dose, viability and mitochondrial superoxide generation. *$P < 0.05$.

a

TNF-α	−	+	+
Niclosamide	−	−	+

Blue: DNA, Red: NF-κB p65

b

Igk mRNA levels

c

Igk FLC secretion

d

IL6	−	+	−	+	−	+
Nic- 1μM	−	−	+	+	−	−
Nic- 2μM	−	−	−	−	+	+

p-STAT3 (Y705)

STAT3

β-actin

Figure 6 Niclosamide inhibits both the NF-κB and STAT3 pathways in myeloma cells. (**a**) UM3 cells were treated with either solvent control or 1 μM niclosamide before the addition of 100 ng/ml TNFα for 15 min. Cytospins were prepared, fixed with paraformaldehyde, stained for NF-κB p65 (red) and counterstained with Hoechst 33342 for DNA. Images are representative of triplicate experiments. (**b**) JJN3 cells were treated overnight with either solvent control, 1 μM niclosamide and/or 10 ng/ml TNFα. RNA was extracted from cells and Igκ levels measured by quantitative real-time PCR. Data shown are mean from $n = 4$ experiments ± s.e.m. (**c**) Supernatant was also harvested from JJN3 cells and secreted FLC protein levels measured by Luminex. Data shown are mean from $n = 4$ experiments ± s.e.m.; *$P < 0.05$. (**d**) JJN3 cells were pretreated with niclosamide at either 1 or 2 μM for 2 h before the addition of 1 μg/ml interleukin 6 (IL6) for 15 min. Total protein was extracted from cells and immunoblotted for total STAT3 protein, Y705 phosphorylated STAT3 with β-actin as a loading control. Images are representative of $n = 3$ experiments.

Discussion

We have demonstrated the potential therapeutic activity of niclosamide against MM both at the level of cell killing and diminution of FLC secretion and that these actions are mediated by mitochondrial disruption and interference in both NF-κB and STAT3 signalling. Niclosamide is an FDA-approved salicylanilide anti-helminthic used in the treatment of intestinal tapeworm infections.[45] It has low toxicity in mammals (oral LD50 in rats, >5000 mg/kg[46,47]) and is inexpensive and readily available. Taken orally, niclosamide exerts its anti-parasitic activity in the intestinal lumen and although it has limited absorption capacity (~10%), micromolar concentrations are achieved in serum after a single oral dose in animals or humans.[46,48] Higher concentrations of ~25 μM were achieved in rats with intravenous application.[47] The peak serum concentration used in our initial screen was 3.2 μM.[46] At this concentration significant anti-proliferative activities were identified in all the MM cell lines tested. Indeed, significant anti-proliferative actions could be detected at concentrations as low as 0.5–1.0 μM in dose-response experiments (Supplementary Figure 2). Niclosamide at similar concentrations, has also been reported to reduce the viability of acute myeloid leukaemia cell lines and primary AML cells without impacting upon the survival of normal CD34 +

haemopoietic stem cells.[38] Similarly we have shown here that niclosamide at doses that are active against MM cells have little affect against PBMCs. Together these findings indicate that niclosamide is unlikely to impact upon normal cells within the therapeutic range that elicits anti-myeloma activity and is therefore unlikely to be significantly myeloablative or immunosuppressive.

Secretion of FLC protein by MM plasma cells is a common feature of MM that frequently causes kidney tubule cast nephropathy and renal failure and accounts for significant morbidity and mortality.[1,49] Renal impairment by monoclonal FLC secretion may also be caused by amyloid deposits as in monoclonal Ig deposition disease and light chain (AL) amyloidosis. The severity of RI is associated with poorer prognosis and rapid reversal of RI with improved survival.[3,9] Our study demonstrated that low micromolar doses of niclosamide reduced both Igκ and Igλ light chain protein production by myeloma cell lines and primary myelomas in vitro (Figures 3a and d). When compared with DEX (a drug clinically used to reduce levels of light chains in MM and other diseases[3,33]) or chemotherapy combinations (MPT, CTD), niclosamide was equally if not more potent (Figure 3). We evaluated whether the actions of niclosamide were transcriptional, possibly through modulation of NF-κB as NF-κB is known to regulate

Igk and not Igλ transcription, or post-transcriptional. Niclosamide induced a reduction in Ig mRNA levels in the κ secreting JJN3 and UM3 cell lines but not in the λ secreting RPMI8226 and L363 cell lines; (Figure 3c) however, TNFα treatment was able to overcome this transcriptional inhibition in UM3 cells (Figure 6b). TNFα treatment was not able to abrogate the niclosamide-mediated reduction in Igk FLC protein secretion in UM3 cells (Figure 6c). This data combined with the observed reductions in intracellular Ig protein in the κ secreting JJN3 line and λ-secreting L363 line (Figure 3b) indicate that niclosamide is acting post-transcriptionally.

The loss of viability of MM cells following niclosamide treatment was associated with markers of both apoptosis and autophagy. Autophagy is a lysosomal pathway responsible for the breakdown of cytoplasmic contents in nutrient-starved cells and is therefore a survival mechanism. In contrast, under certain circumstances autophagic cells may undergo a specific mode of cell death called type II cell death or autophagic cell death. Mammalian target of rapamycin complex 1 (mTORC1) is a critical regulator of autophagy by coupling nutrient sensing to anabolic and catabolic cellular processes.[50] When nutrients are available, mTORC1 is switched on and negatively regulates autophagy.[51] Conversely, nutrient limitation turns off mTORC1 signalling, leading to inhibition of cell growth and stimulation of autophagy. Rapamycin, an irreversible inhibitor of mTORC1, and other rapalogs are under investigation in MM and other haematological malignancies.[52,53] Balgi et al.[34] identified niclosamide as an inhibitor of mTORC1 using a high-throughput screen. These and our data indicate that niclosamide is able to induce autophagy in multiple cancer cell models.

Niclosamide has been demonstrated to regulate multiple cellular pathways including the NF-κB,[38] STAT3,[39] WNT/frizzled1,[54–56] mTORC1[ref.34] and NOTCH[57] signalling pathways. Our data demonstrated that niclosamide is able to affect at least two of the described pathways, which are known to be important in myeloma, the NF-κB pathway and STAT3 signalling (Figure 6). However, we would argue that the major target of niclosamide is the mitochondria. Niclosamide has been demonstrated to uncouple OXPHOS in other human cells[36,37] and induce ROS production in AML cells.[38] Niclosamide treatment of myeloma cells resulted in rapid loss of mitochondrial membrane potential ($\Delta\psi$), with an associated increase in respiration rate consistent with uncoupling of OXPHOS (Figure 4). These changes were associated with the rapid generation of mitochondrial superoxide rather than other ROS species. Furthermore, the generation of mitochondrial superoxide correlated significantly with loss of MM cell viability indicating a critical role for mitochondrial superoxide in niclosamide action (Figure 5). Consistent with this, mitochondrial function is known to regulate both apoptosis and autophagic cell death.[58–60] Further, Chen et al.[58] demonstrated that superoxide, and not other ROS species, is a major regulator of autophagy.

In conclusion, our data indicate that MM cells can be selectively targeted using niclosamide, a drug, which targets the mitochondria and consequently many of the key pathways in myeloma, although also reducing FLC secretion. Importantly, niclosamide is inexpensive, available and likely to have low in vivo toxicity.

Conflict of interest

The authors declare no conflicts of interest.

References

1 Kleber M, Ihorst G, Deschler B, Jakob C, Liebisch P, Koch B et al. Detection of renal impairment as one specific comorbidity factor in multiple myeloma: multicenter study in 198 consecutive patients. Eur J Haematol 2009; 83: 519–527.

2 Clark AD, Shetty A, Soutar R. Renal failure and multiple myeloma: pathogenesis and treatment of renal failure and management of underlying myeloma. Blood Rev 1999; 13: 79–90.

3 Dimopoulos MA, Terpos E, Chanan-Khan A, Leung N, Ludwig H, Jagannath S et al. Renal impairment in patients with multiple myeloma: a consensus statement on behalf of the International Myeloma Working Group. J Clin Oncol 2010; 28: 4976–4984.

4 Rayner HC, Haynes AP, Thompson JR, Russell N, Fletcher J. Perspectives in multiple myeloma: survival, prognostic factors and disease complications in a single centre between 1975 and 1988. Q J Med 1991; 79: 517–525.

5 Augustson BM, Begum G, Dunn JA, Barth NJ, Davies F, Morgan G et al. Early mortality after diagnosis of multiple myeloma: analysis of patients entered onto the United kingdom Medical Research Council trials between 1980 and 2002—Medical Research Council Adult Leukaemia Working Party. J Clin Oncol 2005; 23: 9219–9226.

6 Eleutherakis-Papaiakovou V, Bamias A, Gika D, Simeonidis A, Pouli A, Anagnostopoulos A et al. Renal failure in multiple myeloma: incidence, correlations, and prognostic significance. Leuk Lymphoma 2007; 48: 337–341.

7 Augustson BM, Begum G, Dunn JA, Barth NJ, Davies F, Morgan G et al. Early mortality after diagnosis of multiple myeloma: analysis of patients entered onto the United kingdom Medical Research Council trials between 1980 and 2002—Medical Research Council Adult Leukaemia Working Party. 2005; 23: 9219–9226.

8 Kastritis E, Anagnostopoulos A, Roussou M, Gika D, Matsouka C, Barmparousi D et al. Reversibility of renal failure in newly diagnosed multiple myeloma patients treated with high dose dexamethasone-containing regimens and the impact of novel agents. Haematologica 2007; 92: 546–549.

9 Hutchison CA, Cockwell P, Stringer S, Bradwell A, Cook M, Gertz MA et al. Early reduction of serum-free light chains associates with renal recovery in myeloma kidney. J Am Soc Nephrol 2011; 22: 1129–1136.

10 Child JA, Morgan GJ, Davies FE, Owen RG, Bell SE, Hawkins K et al. High-dose chemotherapy with hematopoietic stem-cell rescue for multiple myeloma. N Engl J Med 2003; 348: 1875–1883.

11 Fermand JP, Katsahian S, Divine M, Leblond V, Dreyfus F, Macro M et al. High-dose therapy and autologous blood stem-cell transplantation compared with conventional treatment in myeloma patients aged 55 to 65 years: long-term results of a randomized control trial from the Group Myelome-Autogreffe. J Clin Oncol 2005; 23: 9227–9233.

12 Harousseau JL, Moreau P. Autologous hematopoietic stem-cell transplantation for multiple myeloma. N Engl J Med 2009; 360: 2645–2654.

13 Anderson KC, Alsina M, Bensinger W, Biermann JS, Chanan-Khan A, Cohen AD et al. NCCN clinical practice guidelines in oncology: multiple myeloma. J Natl Compr Canc Netw 2009; 7: 908–942.

14 Kapoor P, Rajkumar SV, Dispenzieri A, Gertz MA, Lacy MQ, Dingli D et al. Melphalan and prednisone versus melphalan, prednisone and thalidomide for elderly and/or transplant ineligible patients with multiple myeloma: a meta-analysis. Leukemia 2011; 25: 689–696.

15 Turesson I, Velez R, Kristinsson SY, Landgren O. Patterns of improved survival in patients with multiple myeloma in the twenty-first century: a population-based study. J Clin Oncol 2009; 28: 830–834.

16 Singhal S, Mehta J, Desikan R, Ayers D, Roberson P, Eddlemon P et al. Antitumor activity of thalidomide in refractory multiple myeloma. N Engl J Med 1999; 341: 1565–1571.

17 Kumar S, Gertz MA, Dispenzieri A, Lacy MQ, Geyer SM, Iturria NL et al. Response rate, durability of response, and survival after thalidomide therapy for relapsed multiple myeloma. Mayo Clin Proc 2003; 78: 34–39.

18 Weber DM, Chen C, Niesvizky R, Wang M, Belch A, Stadtmauer EA et al. Lenalidomide plus dexamethasone for relapsed multiple myeloma in North America. N Engl J Med 2007; 357: 2133–2142.

19 Orlowski RZ, Nagler A, Sonneveld P, Blade J, Hajek R, Spencer A et al. Randomized phase III study of pegylated liposomal doxorubicin plus bortezomib compared with bortezomib alone in relapsed or refractory multiple myeloma: combination therapy improves time to progression. J Clin Oncol 2007; 25: 3892–3901.

20 Dimopoulos MA, San-Miguel JF, Anderson KC. Emerging therapies for the treatment of relapsed or refractory multiple myeloma. Eur J Haematol 2011; 86: 1–15.

21 Chong CR, Sullivan Jr DJ. New uses for old drugs. Nature 2007; 448: 645–646.

22 DiMasi JA, Hansen RW, Grabowski HG. The price of innovation: new estimates of drug development costs. J Health Econ 2003; 22: 151–185.

23 Morrison PJ, Bradbrook ID, Rogers HJ. Plasma prednisolone levels from enteric and non-enteric coated tablets estimated by an original technique. Br J Clin Pharmacol 1977; 4: 597–603.

24 Newell DR, Calvert AH, Harrap KR, McElwain TJ. Studies on the pharmacokinetics of chlorambucil and prednimustine in man. Br J Clin Pharmacol 1983; 15: 253–258.

25 Bosanquet AG, Gilby ED. Pharmacokinetics of oral and intravenous melphalan during routine treatment of multiple myeloma. Eur J Cancer Clin Oncol 1982; 18: 355–362.

26 Loew D, Schuster O, Graul EH. Dose-dependent pharmacokinetics of dexamethasone. Eur J Clin Pharmacol 1986; 30: 225–230.

27 Chen TL, Kennedy MJ, Anderson LW, Kiraly SB, Black KC, Colvin OM et al. Nonlinear pharmacokinetics of cyclophosphamide and 4-hydroxycyclophosphamide/aldophosphamide in patients with metastatic breast cancer receiving high-dose chemotherapy followed by autologous bone marrow transplantation. Drug Metab Dispos 1997; 25: 544–551.

28 Chen TL, Vogelsang GB, Petty BG, Brundrett RB, Noe DA, Santos GW et al. Plasma pharmacokinetics and urinary excretion of thalidomide after oral dosing in healthy male volunteers. Drug Metab Dispos 1989; 17: 402–405.

29 Piscitelli SC, Figg WD, Hahn B, Kelly G, Thomas S, Walker RE. Single-dose pharmacokinetics of thalidomide in human immunodeficiency virus-infected patients. Antimicrob Agents Chemother 1997; 41: 2797–2799.

30 Canfell C, Sadee W. Methotrexate and 7-hydroxymethotrexate: serum level monitoring by high-performance liquid chromatography. Cancer Treat Rep 1980; 64: 165–169.

31 Dispenzieri A, Kyle R, Merlini G, Miguel JS, Ludwig H, Hajek R et al. International Myeloma Working Group guidelines for serum-free light chain analysis in multiple myeloma and related disorders. Leukemia 2009; 23: 215–224.

32 Gertz MA, Lacy MQ, Lust JA, Greipp PR, Witzig TE, Kyle RA. Phase II trial of high-dose dexamethasone for previously treated immunoglobulin light-chain amyloidosis. Am J Hematol 1999; 61: 115–119.

33 Gertz MA, Lacy MQ, Lust JA, Greipp PR, Witzig TE, Kyle RA. Phase II trial of high-dose dexamethasone for untreated patients with primary systemic amyloidosis. Med Oncol 1999; 16: 104–109.

34 Balgi AD, Fonseca BD, Donohue E, Tsang TC, Lajoie P, Proud CG et al. Screen for chemical modulators of autophagy reveals novel therapeutic inhibitors of mTORC1 signaling. PLoS One 2009; 4: e7124.

35 Pampori NA, Singh G, Srivastava VM. Energy metabolism in Cotugnia digonopora and the effect of anthelmintics. Mol Biochem Parasitol 1984; 11: 205–213.

36 Curnock AP, Thomson TA, Westwood R, Kuo EA, Williamson RA, Yea CM et al. Inhibition of stimulated Jurkat cell adenosine 3′,5′-cyclic monophosphate synthesis by the immunomodulatory compound HR325. Biochem Pharmacol 2001; 61: 227–235.

37 MacDonald ML, Lamerdin J, Owens S, Keon BH, Bilter GK, Shang Z et al. Identifying off-target effects and hidden phenotypes of drugs in human cells. Nat Chem Biol 2006; 2: 329–337.

38 Jin Y, Lu Z, Ding K, Li J, Du X, Chen C et al. Antineoplastic mechanisms of niclosamide in acute myelogenous leukemia stem cells: inactivation of the NF-kappaB pathway and generation of reactive oxygen species. Cancer Res 2010; 70: 2516–2527.

39 Ren X, Duan L, He Q, Zhang Z, Zhou Y, Wu D et al. Identification of niclosamide as a new small-molecule inhibitor of the STAT3 signaling pathway. ACS Med Chem Lett 2010; 1: 454–459.

40 Bhardwaj A, Sethi G, Vadhan-Raj S, Bueso-Ramos C, Takada Y, Gaur U et al. Resveratrol inhibits proliferation, induces apoptosis, and overcomes chemoresistance through down-regulation of STAT3 and nuclear factor-kappaB-regulated antiapoptotic and cell survival gene products in human multiple myeloma cells. Blood 2007; 109: 2293–2302.

41 Catlett-Falcone R, Landowski TH, Oshiro MM, Turkson J, Levitzki A, Savino R et al. Constitutive activation of Stat3 signaling confers resistance to apoptosis in human U266 myeloma cells. Immunity 1999; 10: 105–115.

42 Conticello C, Giuffrida R, Adamo L, Anastasi G, Martinetti D, Salomone E et al. NF-kappaB localization in multiple myeloma plasma cells and mesenchymal cells. Leuk Res 2011; 35: 52–60.

43 Junker S, Lamm M, Nielsen V, Matthias P. Extinction of immunoglobulin gene expression in B cells upon fusion with HeLa cells is preceded by rapid nuclear depletion of essential transcription factors and is accompanied by widespread inactivation of genes expressed in a B cell-specific manner. J Cell Sci 1997; 110 (Part 20): 2579–2587.

44 Kawano M, Hirano T, Matsuda T, Taga T, Horii Y, Iwato K et al. Autocrine generation and requirement of BSF-2/IL-6 for human multiple myelomas. Nature 1988; 332: 83–85.

45 Weinbach EC, Garbus J. Mechanism of action of reagents that uncouple oxidative phosphorylation. Nature 1969; 221: 1016–1018.

46 WHO. Specifications and Evaluations for Public Health Pesticides: Niclosamide. World Health Organization 2002; Available from http://www.wpro.who.int/NR/rdonlyres/7E9635EA-82C3-4D8C-8938-03F26D432E30/0/NiclosamideWHOSpecificationsandEvaluationsforPublicHealthPesticides.pdf.

47 Chang YW, Yeh TK, Lin KT, Chen WC, Yao HT, Lan SJ et al. Pharmacokinetics of anti-SARS-CoV agent niclosamide and Its analogs in rats. J Food Drug Anal 2006; 14: 329–333.

48 Merschjohann K, Steverding D. In vitro trypanocidal activity of the anti-helminthic drug niclosamide. Exp Parasitol 2008; 118: 637–640.

49 Dimopoulos MA, Terpos E. Renal insufficiency and failure. Hematol Am Soc Hematol Educ Program 2011; 2010: 431–436.

50 Wullschleger S, Loewith R, Hall MN. TOR signaling in growth and metabolism. Cell 2006; 124: 471–484.

51 Kundu M, Thompson CB. Autophagy: basic principles and relevance to disease. Annu Rev Pathol 2008; 3: 427–455.

52 Gera J, Lichtenstein A. The mammalian target of rapamycin pathway as a therapeutic target in multiple myeloma. Leuk Lymphoma 2011; 52: 1857–1866.

53 Vu C, Fruman DA. Target of rapamycin signaling in leukemia and lymphoma. Clin Cancer Res 2010; 16: 5374–5380.

54 Chen M, Wang J, Lu J, Bond MC, Ren XR, Lyerly HK et al. The anti-helminthic niclosamide inhibits Wnt/Frizzled1 signaling. Biochemistry 2009; 48: 10267–10274.

55 Chen W, Chen M, Barak LS. Development of small molecules targeting the Wnt pathway for the treatment of colon cancer: a high-throughput screening approach. Am J Physiol Gastrointest Liver Physiol 2010; 299: G293–G300.

56 Osada T, Chen M, Yang XY, Spasojevic I, Vandeusen JB, Hsu D et al. Antihelminth compound niclosamide downregulates Wnt signaling and elicits antitumor responses in tumors with activating APC mutations. Cancer Res 2011; 71: 4172–4182.

57 Wang AM, Ku HH, Liang YC, Chen YC, Hwu YM, Yeh TS. The autonomous notch signal pathway is activated by baicalin and baicalein but is suppressed by niclosamide in K562 cells. J Cell Biochem 2009; 106: 682–692.

12

58 Chen Y, Azad MB, Gibson SB. Superoxide is the major reactive oxygen species regulating autophagy. *Cell Death Differ* 2009; **16**: 1040–1052.

59 Tiwari M, Lopez-Cruzan M, Morgan WW, Herman B. Loss of caspase-2 dependent apoptosis induces autophagy following mitochondria oxidative stress in primary cultures of young-adult cortical neurons. *J Biol Chem* 2011; **286**: 8493–8506.

60 Lemasters JJ, Qian T, Bradham CA, Brenner DA, Cascio WE, Trost LC *et al*. Mitochondrial dysfunction in the pathogenesis of necrotic and apoptotic cell death. *J Bioenerg Biomembr* 1999; **31**: 305–319.

Supplementary Information accompanies the paper on Blood Cancer Journal website (http://www.nature.com/bcj)